

A Prediction-Based Reversible Watermarking for MRI Images

Nuha Omran Abokhdair, Azizah Bt Abdul Manaf

Abstract—Reversible watermarking is a special branch of image watermarking, that is able to recover the original image after extracting the watermark from the image. In this paper, an adaptive prediction-based reversible watermarking scheme is presented, in order to increase the payload capacity of MRI medical images. The scheme divides the image into two parts, Region of Interest (ROI) and Region of Non-Interest (RONI). Two bits are embedded in each embeddable pixel of RONI and one bit is embedded in each embeddable pixel of ROI. The experimental results demonstrate that the proposed scheme is able to achieve high embedding capacity. This is mainly caused by two reasons. First, the pixels that were excluded from data embedding due to overflow/underflow are used for data embedding. Second, large location map that need to be added to watermark data as overhead is eliminated and thus lower data embedding capacity is prevented. Moreover, the scheme provides good visual quality to the watermarked image.

Keywords—Medical image watermarking, reversible watermarking, Difference Expansion, Prediction-Error Expansion.

I. INTRODUCTION

NOWADAYS the distribution and communication of medical information among health care providers and telemedicine systems are becoming increasingly crucial. One of the most significant types of medical information is Magnetic Resonance Imaging (MRI), where the transmission of this type of medical images over wire and wireless networks is a daily routine in medical life [1], [2]. On the other hand, the distribution of medical images over unsecured network channels, such as internet, produces potential risk of information disclosure to an unauthorized entity, where it is intentional or not intentional. A manipulation of the context of the medical image is a possible consequence of this, which may cause misdiagnosis [1], [3].

One of the techniques that used to protect MRI medical images from unauthorized access is medical image watermarking. Medical image watermarking is used to insert the related electronic patient record (EPR) into the medical image in order to avoid detachment of EPR from its corresponding image. Moreover, medical image watermarking can be also used for authentication and tamper detection purpose, in order to identify the source of the image and to detect and localize any manipulation of the image. As a consequence, much data must be hidden inside the image and

the embedding capacity must be high enough to accommodate the payload [4]-[7].

On the other hand, in medical images, even a minor distortion of the image caused by watermarking is prohibited, because this may affect the diagnosis negatively. To overcome this problem, reversible watermarking is used. The main feature of reversible watermarking is that an exact copy of the original image can be recovered, if the watermarked image is considered authentic [5]-[10].

Several reversible watermarking techniques have been proposed, e.g. difference expansion technique (DE) [10], histogram shifting technique [11], [12], prediction-error expansion technique (PEE) [13]-[16], etc. Among these reversible schemes, the main advantage of PEE is that PEE has the potential to well exploit the spatial redundancy in natural images [14]. PEE was introduced by Thodi and Rodriguez in [13] as an improvement of DE technique of Tian [10]. Where, prediction-error histogram is used for expansion embedding rather than difference value [17].

The mechanism of PEE-based embedding can be described as follows. At the beginning, image pixels are predicted to get the prediction-error histogram which is a Laplacian-like distribution centered at zero. Then, a capacity-parameter is determined according to the capacity, in order to get the inner region and outer region. Finally, the prediction-error of each pixel of inner region is expanded to carry 1 bit of the watermark, and the prediction-error of pixels of outer region are shifted to avoid ambiguity. In summary, PEE is able to embed a large payload by exploiting the prediction-error histogram, and control the distortion by simultaneously using expansion embedding and histogram shifting [13], [14].

In this paper, we aim at obtaining a reversible data hiding scheme based on adaptive PEE technique that can achieve high embedding capacity for medical images by concealing the payload with different embedding strength in ROI and RONI. In addition, the proposed scheme introduces less distortion to the ROI of the medical image, which leads to improve the transparency of the proposed method.

II. THE PROPOSED SCHEME

The embedding process and extraction and recovery process of the proposed watermarking algorithm for medical image is described as follows:

A. Embedding Process

The embedding process is as follows:

- 1) The image is divided into ROI and RONI, the ROI is selected and defined as a polygon by the physician.

Nuha Omran Abokhdair is with the Faculty of Computer Science and Information System, Universiti Teknologi Malaysia, 54100 Kuala Lumpur, Malaysia (e-mail: Abo_khdeir@yahoo.com).

Azizah Bt Abdul Manaf is with the Advanced Informatics School, Universiti Teknologi Malaysia, 54100 Kuala Lumpur, Malaysia (e-mail: azizah07@citycampus.utm.my).

- 2) The host image I is scanned in raster scan order excluding the first row and first column. Each pixel is predicted by the following formula (1):

$$I'(x, y) = \left\lfloor \frac{I(x-1, y) + I(x, y-1)}{2} \right\rfloor \quad (1)$$

where, $\lfloor \cdot \rfloor$ denotes the floor function which rounds the elements to the least nearest integer. The prediction error is the calculated using (2):

$$e = |I(x, y) - I'(x, y)| \quad (2)$$

- 3) For each RONI pixel, according to a predefined threshold T' , e is classified as two conditions which are $e \leq T'$ and $e > T'$.

Expandable pixel of RONI: If $e \leq T'$, then the watermarked value is taken as (3):

$$I^w(x, y) = \begin{cases} I'(x, y) + 4e + b, & \text{if } I'(x, y) \leq I(x, y), \\ I'(x, y) - 4e - b, & \text{otherwise.} \end{cases} \quad (3)$$

where $b \in \{0, 1, 2, 3\}$ represents two bits.

Shiftable pixels of RONI: If $e > T'$, the prediction-error is simply shifted by δ' with no embedded data and the watermarked value is calculated by (4):

$$I^w(x, y) = \begin{cases} I'(x, y) + \delta', & \text{if } I'(x, y) \leq I(x, y), \\ I'(x, y) - \delta', & \text{otherwise.} \end{cases} \quad (4)$$

where $\delta' = 3T' + 3$.

- 4) For each ROI pixel, according to a predefined threshold T , the prediction error, e , is categorized into two cases which are $e \leq T$ and $e > T$.

Expandable pixel of ROI: If $e \leq T$, then the watermarked pixel is computed by (5):

$$I^w(x, y) = \begin{cases} I'(x, y) + 2e + b, & \text{if } I'(x, y) \leq I(x, y), \\ I'(x, y) - 2e - b, & \text{otherwise.} \end{cases} \quad (5)$$

where $b \in \{0, 1\}$ represents one bit.

Shiftable pixels of ROI: If $e > T$, the watermarked pixel is calculated by shifting the original pixel by δ with no embedded data, refer to (6):

$$I^w(x, y) = \begin{cases} I'(x, y) + \delta, & \text{if } I'(x, y) \leq I(x, y), \\ I'(x, y) - \delta, & \text{otherwise.} \end{cases} \quad (6)$$

where $\delta = T + 1$.

- 5) The parameters such as thresholds, T and T' , and the vertexes of the ROI polygon should be communicated to decoder for blind extraction, and we will embed them into host image as auxiliary information.

B. Extraction and Recovery Process

The extraction and recovery process is explained as below:

- 1) Extract the auxiliary information from the host image. This information includes the capacity thresholds and the ROI polygon vertexes, which are used to define the ROI and RONI of the watermarked medical image as in the embedding process.
- 2) The watermarked image is scanned in raster scan order and the prediction $I'(x, y)$ is computed. This value is exactly the same as the one used by encoder. The prediction error is calculated by (7):

$$e^w = |I^w(x, y) - I'(x, y)| \quad (7)$$

- 3) For each RONI pixel, according to a predefined threshold T' , e^w is classified as two conditions which are $e^w \leq 4T' + 3$ and $e^w > 4T' + 3$.

Expandable pixel of RONI: If $e^w \leq 4T' + 3$, then the embedded data (2 bits) is taken as in (8):

$$b = e^w - 4 \left\lfloor \frac{e^w}{4} \right\rfloor \quad (8)$$

And the original pixel value is calculated by (9):

$$I(x, y) = \begin{cases} I'(x, y) + \left\lfloor \frac{e^w}{4} \right\rfloor, & \text{if } I'(x, y) \leq I^w(x, y), \\ I'(x, y) - \left\lfloor \frac{e^w}{4} \right\rfloor, & \text{otherwise.} \end{cases} \quad (9)$$

Shiftable pixels of RONI: If $e^w > 4T' + 3$, no data will be extracted, And the original pixel value is computed by (10):

$$I(x, y) = \begin{cases} I'(x, y) + \delta', & \text{if } I'(x, y) \leq I^w(x, y), \\ I'(x, y) - \delta', & \text{otherwise.} \end{cases} \quad (10)$$

- 4) For each ROI pixel, according to a predefined threshold T , the prediction error, e^w , is categorized into two cases which are $e^w \leq 2T + 1$ and $e^w > 2T + 1$.

Expandable pixel of ROI: If $e^w \leq 2T + 1$, then the embedded data (1 bits) is taken as in (11):

$$b = e^w - 2 \left\lfloor \frac{e^w}{2} \right\rfloor \quad (11)$$

And the original pixel value is determined by (12):

$$I(x, y) = \begin{cases} I'(x, y) + \left\lfloor \frac{e^w}{2} \right\rfloor, & \text{if } I'(x, y) \leq I^w(x, y), \\ I'(x, y) - \left\lfloor \frac{e^w}{2} \right\rfloor, & \text{otherwise.} \end{cases} \quad (12)$$

Shiftable pixels of ROI: If $e^w > 2T + 1$, then no data will be extracted, And the original pixel value is computed by (13):

$$I(x, y) = \begin{cases} I'(x, y) + \delta, & \text{if } I'(x, y) \leq I^w(x, y), \\ I'(x, y) - \delta, & \text{otherwise.} \end{cases} \quad (13)$$

C. Overflow and Underflow Prevention

In this phase, overflow and underflow conditions are avoided, in order to guarantee that the host image is suitable for embedding. Overflow and underflow problem occurs when the watermark embedding process cause the pixels in boundaries overstepping the boundaries.

“MRI DICOM images are generally stored using 16 bits per pixel and imaging modalities usually do not produce images that utilize the full range of pixel values” [15]. For instance, the pixel values of MRI1 in Fig. 1 range from 0 to 65535, where, the highest pixel value is only 1080. Moreover, most of the boundary pixels’ values are close to 0.

Therefore, to prevent underflow, the proposed scheme shifts the pixels’ values of ROI and RONI by $\delta+1$ and $\delta'+1$, respectively, in a way does not make any pixel exceed the maximum value of the pixel.

At the end of extraction process, the histograms of ROI and RONI are shifted back to their original values by $-(\delta+1)$ and $-(\delta'+1)$, respectively.

III. EXPERIMENTAL RESULTS

Three 16-bit DICOM MRI images with size of 512x512 are used to test the proposed scheme. A random bit stream generated as a watermark to be embedded in every image. The capacity parameter T’ is taken as $\lceil T/3 \rceil$ to ensure that each pixel value is modified at most by T, and T is taken as the smallest threshold that can provide enough expandable pixels to embed the payload. To evaluate the imperceptibility, Peak Signal to Noise Ratio (PSNR) is used as the most common measure. The PSNR formula is defined as in (14).

$$PSNR = 10 \log_{10} \frac{(I_{max})^2}{MSE} \text{ dB} \quad (14)$$

where I_{max} is the maximum pixel value in the image and MSE is the mean squared error between the watermarked image and the original image. The hiding capacity is measured as the number of bits embedded per pixel. The watermark obtained from the watermarked image, and the equality between the original image and the retrieved one has verified the reversibility of this scheme.

Table I and Fig. 1 summarize the performance results of the proposed scheme on the three MRI images. The experimental results demonstrate that the maximum hiding capacity achieved by the scheme is approximately 1.5 bpp for all images with PSNR value exceeds 47 db.

TABLE I
THE MAXIMUM HIDING CAPACITY OF THE PROPOSED SCHEME

Image	Maximum embedding capacity (bpp)	Payload (bits)	PSNR (db)
MRI1	1.55	407,737	55.77
MRI2	1.57	413,373	55.91
MRI3	1.509	395,728	47.97

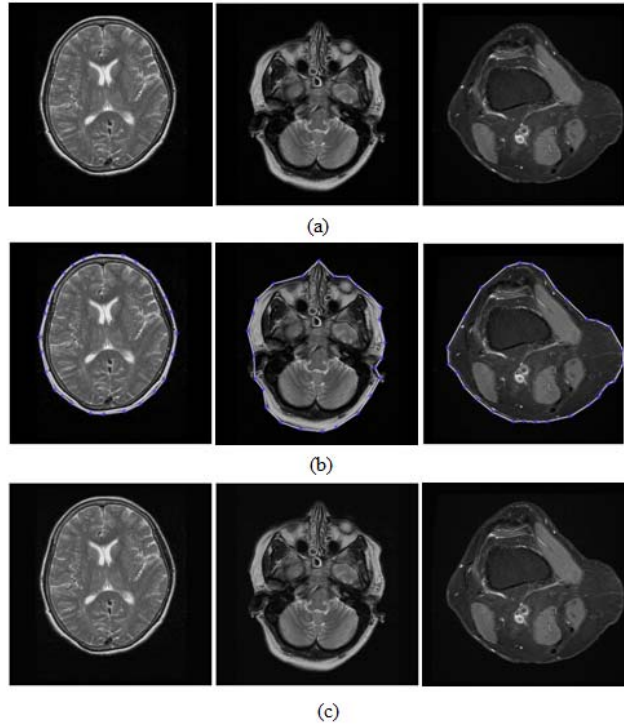


Fig. 1 Results of embedding the watermark. (a) Original images (MRI1, MRI2, and MRI3). (b) Selected ROI. (c) Watermarked images

The degradation in the watermarked images’ visual quality with respect to the original images, in terms of PSNR, is tested by embedding different capacities, which vary from 0.1bpp to its maximum with step size 0.1, in the test images. Although the three images were of the same size and bit depth, Fig. 2 shows that the PSNR value of MRI1 and MRI2 is better than the corresponding value of MRI3. This is mainly because the proposed scheme is image-dependant scheme.

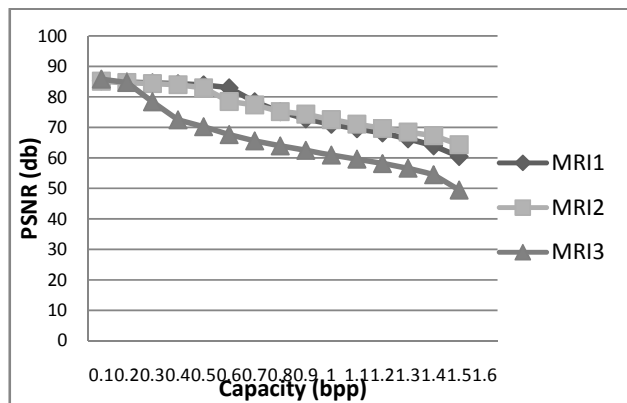


Fig. 2 Distortion for images tested by the proposed scheme at varying embedding capacity

In Fig. 3, MRI1 image is used to compare the performance of the proposed scheme with Tian scheme [10], Alattar scheme [18], Al-Qershi scheme1 [5] and Al-Qershi scheme2

[5]. From the figure, it is obvious that the proposed method has higher embedding capacity up to 1.5 bpp, while Tian scheme and Alattar schemes can only achieve 0.3 bpp and both Al-Qershi schemes can achieve 0.5bpp.

According to the visual quality, the PSNR values of the proposed method are higher than the corresponding PSNR values of the other conventional methods.

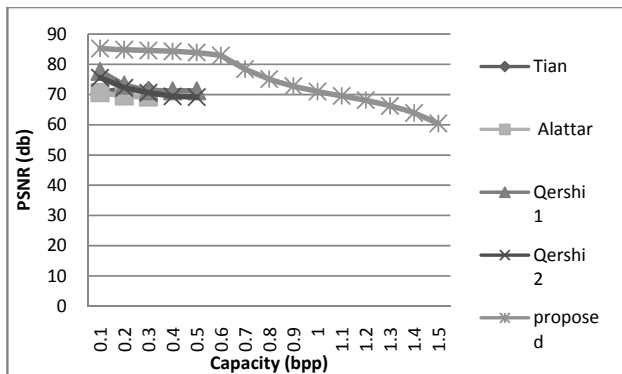


Fig. 3 Performance comparison between the proposed scheme and schemes of Tian [10], Alattar [18] and Al-Qershi [5]

IV. CONCLUSION

In this paper, a novel reversible watermarking scheme for MRI images has been proposed. Adaptive prediction expansion error technique is used to embed two bits in the expandable pixels of RONI and one bit in the expandable pixels of ROI, in order to introduce less distortion in ROI. The overflow/underflow problem is solved and location map is eliminated in this scheme. This allows the scheme to conceal high embedding capacity with good visual quality.

According to the experimental results, the proposed reversible watermarking scheme yields superior performance to the other state-of-art schemes. It provides higher hiding capacity and better image fidelity.

REFERENCES

- [1] W. Puech, "Image Encryption and Compression for Medical Image Security" presented at the Image Processing Theory, Tools and Applications, Sousse 2008.
- [2] N. O. Abokhdair, et al., "Integration of chaotic map and confusion technique for color medical image encryption," in Digital Content, Multimedia Technology and its Applications (IDC), 2010 6th International Conference on, 2010, pp. 20-23.
- [3] L. Eugene Y.S, "11 - Data Security and Protection for Medical Images," in Biomedical Information Technology, F. David Dagan, Ed., ed Burlington: Academic Press, 2008, pp. 249-257.
- [4] O. M. Al-Qershi and B. E. Khoo, "Authentication and Data Hiding Using a Reversible ROI-based Watermarking Scheme for DICOM Images," presented at the Proceedings of International Conference on Medical Systems Engineering (ICMSE), 2009.
- [5] O. M. Al-Qershi and B. E. Khoo, "High capacity data hiding schemes for medical images based on difference expansion," J. Syst. Softw., vol. 84, pp. 105-112, 2011.
- [6] O. Al-Qershi and B. Khoo, "Authentication and Data Hiding Using a Hybrid ROI-Based Watermarking Scheme for DICOM Images," Journal of Digital Imaging, vol. 24, pp. 114-125, 2011.
- [7] M. K. Kundu and S. Das, "Lossless ROI Medical Image Watermarking Technique with Enhanced Security and High Payload Embedding," presented at the Proceedings of the 2010 20th International Conference on Pattern Recognition, 2010.
- [8] L. Kamstra and H. J. A. M. Heijmans, "Reversible data embedding into images using wavelet techniques and sorting," Trans. Img. Proc., vol. 14, pp. 2082-2090, 2005.
- [9] S. M. Abdullah, et al., "Capacity and quality improvement in reversible image watermarking approach," in Networked Computing and Advanced Information Management (NCM), 2010 Sixth International Conference on, 2010, pp. 81-85.
- [10] J. Tian, "Reversible data embedding using a difference expansion," Circuits and Systems for Video Technology, IEEE Transactions on, vol. 13, pp. 890-896, 2003.
- [11] Z. Ni, et al., "Reversible data hiding," Circuits and Systems for Video Technology, IEEE Transactions on, vol. 16, pp. 354-362, 2006.
- [12] S. K. Lee, et al., "Reversible Image Authentication Based on Watermarking," in Multimedia and Expo, 2006 IEEE International Conference on, 2006, pp. 1321-1324.
- [13] D. M. Thodi and J. J. Rodríguez, "Expansion embedding techniques for reversible watermarking," Image Processing, IEEE Transactions on, vol. 16, pp. 721-730, 2007.
- [14] X. Li, et al., "Efficient reversible watermarking based on adaptive prediction-error expansion and pixel selection," IEEE Trans Image Process, 2011.
- [15] C. Tan, et al., "Security Protection of DICOM Medical Images Using Dual-Layer Reversible Watermarking with Tamper Detection Capability," Journal of Digital Imaging, vol. 24, pp. 528-540, 2011.
- [16] C.-F. Lee, et al., "Embedding capacity raising in reversible data hiding based on prediction of difference expansion," Journal of Systems and Software, vol. 83, pp. 1864-1872, 2010.
- [17] Y. Luo, "Reversible image water marking based on prediction-error expansion and compensation," 2011, pp. 1-6.
- [18] A. M. Alattar, "Reversible watermark using difference expansion of quads," in Acoustics, Speech, and Signal Processing, 2004. Proceedings. (ICASSP '04). IEEE International Conference on, 2004, pp. 77-80.